

c.2



Lawrence Berkeley Laboratory

UNIVERSITY OF CALIFORNIA

RECEIVED
LAWRENCE
BERKELEY LABORATORY

SEP 30 1982

LIBRARY AND
DOCUMENTS SECTION

Materials & Molecular Research Division

To be published in Surface Science

THE GROWTH AND CHEMISORPTIVE PROPERTIES OF Ag AND
Au MONOLAYERS ON PLATINUM SINGLE CRYSTAL SURFACES:
AN AES, TDS, AND LEED STUDY

P.W. Davies, M.A. Quinlan, and G.A. Somorjai

June 1982

TWO-WEEK LOAN COPY

*This is a Library Circulating Copy
which may be borrowed for two weeks.
For a personal retention copy, call
Tech. Info. Division, Ext. 6782.*



LBL-12946
c.2

DISCLAIMER

This document was prepared as an account of work sponsored by the United States Government. While this document is believed to contain correct information, neither the United States Government nor any agency thereof, nor the Regents of the University of California, nor any of their employees, makes any warranty, express or implied, or assumes any legal responsibility for the accuracy, completeness, or usefulness of any information, apparatus, product, or process disclosed, or represents that its use would not infringe privately owned rights. Reference herein to any specific commercial product, process, or service by its trade name, trademark, manufacturer, or otherwise, does not necessarily constitute or imply its endorsement, recommendation, or favoring by the United States Government or any agency thereof, or the Regents of the University of California. The views and opinions of authors expressed herein do not necessarily state or reflect those of the United States Government or any agency thereof or the Regents of the University of California.

THE GROWTH AND CHEMISORPTIVE PROPERTIES OF Ag AND Au MONOLAYERS ON
 PLATINUM SINGLE CRYSTAL SURFACES: AN AES, TDS, AND LEED STUDY

P.W. Davies*, M.A. Quinlan, and G.A. Somorjai

Materials and Research Division, Lawrence Berkeley Laboratory
 and
 Department of Chemistry, University of California, Berkeley, CA 94720

Abstract

The growth and chemisorptive properties of monolayer films of Ag and Au deposited on both the Pt(111) and the stepped Pt(553) surfaces were studied using Auger electron spectroscopy (AES), thermal desorption spectroscopy (TDS), and low energy electron diffraction (LEED). AES studies indicate that the growth of Au on the Pt(111), and Pt(553) and Ag on the Pt(111) proceeds via a Stranski-Krastanov mechanism, whereas the growth of Ag on the Pt(553) surface follows a Volmer-Weber mechanism.

Au dissolves into the Pt crystal bulk at temperatures >800 K, whereas Ag desorbs at temperatures >900 K. TDS studies of Ag-covered Pt surfaces indicate that the Ag-Pt bond (283 kJ mol^{-1}) is $\sim 25 \text{ kJ mol}^{-1}$ stronger than the Ag-Ag bond (254 kJ mol^{-1}). On the Pt(553) surface the Au atoms are uniformly distributed between terrace and step sites, but Ag preferentially segregates to the terraces.

The decrease in CO adsorption on the Pt crystal surfaces is in direct proportion to the Ag or Au coverage. No CO adsorption could be detected for Ag or Au coverages above one monolayer at 300 K and 10^{-8} torr. The heat of adsorption of CO on Pt is unaltered by the presence of Ag or Au.

*Permanent address: Bendix Advanced Technology Center
 Columbia, MD 21045

This work was supported by the Director, Office of Energy Research, Office of Basic Energy Sciences, Materials Sciences Division of the U.S. Department of Energy under Contract DE-AC03-76SF00098; and by a grant from the Dow Chemical Company.

1. Introduction

Controlled modification of the chemical properties of metal surfaces by the addition of a second metallic component has long been the goal of the surface chemist. Ferrous metals may be rendered impervious to chemical corrosion by surface plating with a more electropositive metal (Zn, for example) or by alloying with a more noble metal (e.g. addition of Cr in the manufacture of stainless steels). Multicomponent alloy catalysts exhibit properties which are in many ways superior to any of the individual components, a fact that is evidenced by their widespread use throughout the chemical industry.¹

One of the more successful classes of catalysts that are used in hydrocarbon conversion reactions contain two metal components: a catalytically active transition metal (i.e. Pt, Ir, Ru, Pd) in combination with a catalytically less active metal from the Group IB of the periodic table (Au, Ag, or Cu). This group of catalysts, when properly dispersed, can catalyze reactions at higher rates and are less prone to poisoning reactions and generally exhibit higher selectivities.¹⁻³

It is essential to gain a better understanding of how the structure and composition of alloy surfaces influence their chemical properties in order to be able to predict and tailor their catalytic properties. For this reason we have embarked on a study of the silver-platinum and the gold-platinum surfaces. We have deposited controlled amounts of the Group IB metals Au and Ag onto well-defined Pt single crystal substrates. A combination of Auger electron spectroscopy (AES), low energy electron diffraction (LEED), and thermal desorption spectroscopy (TDS) was then used to characterize the morphology and composition of the metallic adlayers.

The adsorption and desorption of carbon monoxide was used as a probe to determine the influence of Au and Ag on the known chemisorptive properties of Pt. Two different Miller index Pt single crystals were used to determine the effect of surface structure on the observed properties. We examined the atomically flat, hexagonally close-packed Pt(111) surface and the stepped Pt(553) surface. The geometries of the two surfaces are shown schematically in Fig.1. A fcc (553) surface may be regarded as a staggered array of (111) planes separated by monatomic height steps of (111) orientation resulting in a step density of 20%.

Our layer growth and CO adsorption studies both indicate that Ag adsorbs preferentially on terrace sites. In contrast, Au adsorbs uniformly at both step and terrace sites. Upon heating, the Au adlayers dissolved into the crystal bulk, whereas Ag desorbs at temperatures >900 K and could be detected by mass spectrometry. Analysis of AMU 107 thermal desorption spectra indicated that the Pt-Ag bond was about $25 \text{ kJ}\cdot\text{mol}^{-1}$ stronger than the Ag-Ag bond. While the CO coverage decreased linearly with increasing Ag or Au surface concentration, the heat of adsorption of the molecule remained by-and-large unaltered.

2. Experimental

All experiments were performed in an ion-pumped stainless steel UHV system of conventional design. Analytical probes included a 4-grid LEED optics, used for both LEED observations and Auger electron analysis, a glancing incidence Auger electron gun, and a UTI-100C mass spectrometer placed at close (~ 5 cm) line-of-sight to the specimen face, thus maximizing the system's sensitivity to desorbing species.

A modified specimen manipulator, allowing both Pt single crystal specimens to be mounted simultaneously in the system, enabled direct comparisons of

their properties to be made. The specimens could be independently heated by conduction from resistively heated 0.3 mm Ta support wires. Specimen temperature was monitored by Chromel-Alumel thermocouples spot welded to the rear face of each crystal. Prior to each experiment, surface contamination was removed by Ar⁺ ion bombardment. Residual carbon was chemically removed by heat treating the specimens in 10⁻⁷ torr of oxygen.

Both the Ag and Au adlayers were deposited on the crystal surfaces from a flux produced by an electrically heated Knudsen oven mounted at a distance of ~ 15 cm from the specimen faces. After an initial outgassing, high purity fluxes of constant intensities could be maintained over periods of several hours. The intensities of the fluxes impinging on the specimen faces were typically ~ 0.6 x10¹² and ~ 1.0x10¹³ atoms minute⁻¹cm⁻² for Au and Ag, respectively. Auger analysis indicated that this flux was uniform over the entire specimen area.

3. Auger calibration of adlayer coverages and determination of growth morphology.

Prior to the investigation of CO adsorption on the Ag and Au covered Pt surface, it was necessary to determine the morphology of adlayer growth and also to determine an Auger calibration for the adlayer coverage. Fig.2 illustrates the various growth morphologies which may be adopted by a vapor condensing onto a substrate and also shows the predicted variation in Auger signal intensity from both the substrate and adsorbate atoms as a function of time of exposure to a constant adsorbate flux (AST plots). These various crystal growth models were proposed for substrates with one type of adsorption site. It is not clear how they may be altered for substrate surfaces with high step density.

1. Frank-Van der Merwe growth behavior

Growth proceeds layer-by-layer, and the AST plots consists of a series of straight line segments with breaks occurring at the transition between

the completion of one layer and the commencement of the next layer. Gallon⁴ has demonstrated that the break will be most apparent during the transition between the first and second monolayers. In addition, if the Auger intensity from an infinite slab of substrate, an infinite slab of adsorbate, and the Auger intensity from a single monolayer of adsorbate are known, the entire variation of the AST plot may be simply devised.

2. Volmer-Weber growth behavior

Growth proceeds via the formation of three-dimensional crystallites. The AST plots will show a smooth variation whose form is dependent on the exact shape and size of the crystallites.

3. Stranski-Krastanov growth behavior

An intermediate case in which a complete first monolayer is formed to be followed by the development of three-dimensional crystallites. The AST plot show a linear variation up to the completion of the first monolayer to be followed by a smooth variation up to a saturation value.

4. Results

4.1 Growth of and properties of Ag on Pt(111) and Pt(553)

Auger spectra obtained from the clean Pt(111) and a surface covered with $\sim 0.8 \theta$ Ag are shown in Fig.3. The transitions at 64 V and at 351 V can be seen to rise solely from Pt and Au, respectively, and therefore their peak-to-peak heights could be used directly in the construction of the AST plots. The relative amount of Ag deposited was assumed to be proportional to the time of exposure to the silver flux.

The AST plots for Ag growth on the Pt(111) and Pt(533) surfaces are presented in Figs. 4a and 4b, respectively. The plot for the Pt(111) surface shows a linear portion followed by a smooth variation to saturation value,

indicative of an Stranski-Krastanov growth mechanism. The break in this plot is identified with the completion of the first monolayer and thus provides the basis for an Auger calibration.

Confirmation of the Stranski-Krastanov growth mechanism is provided by plotting the continuation of the AST plot beyond the first monolayer expected from the Frank-Van der Merwe growth mechanism. As expected, due to the poorer shielding of three-dimensional crystallites relative to the same amount of adsorbate material arranged as single monolayers, the Auger signal intensities of Ag and Pt are, respectively, below and above that predicted from the Frank-Van der Merwe model.

A different behavior is indicated for Ag growth on the Pt(553) surface. A smooth variation in both the Ag 361/365 V and the Pt 64 V signals at all coverages is indicative of a Volmer-Weber growth mechanism. For a system displaying this growth it is not possible to derive independently the exact adsorbate coverages. However, since Ag desorbed completely from the Pt single crystal surfaces upon heating >900 K, it was possible to use the AMU 107 thermal desorption yields from both crystals to compare Ag coverages on the calibrated Pt(111)/Ag system with coverages for the uncalibrated Pt(533)/Ag system. Coverage values derived in this way are used in the Pt(553)/Ag AST plot.

AMU 107 TDS results from Ag-covered Pt(111) and Pt(553) surfaces are presented in Figs. 5a and 5b. Up to an initial Ag coverage of one monolayer, a single, slightly asymmetric desorption peak centered at ~ 1080 K is observed from the Pt(111) substrate. At coverages >1 monolayer a second, lower temperature peak develops and becomes the dominant desorption feature at coverages >2 monolayers. The higher temperature peak is therefore identified with desorption from the first monolayer, while the lower temperature peak is identified with desorption from subsequent monolayers. Assuming first-order desorption

kinetics for the higher temperature peak and applying the Redhead⁵ formula using a pre-exponential of 10^{13}sec^{-1} , appropriate for a surface layer of mobile species, an activation energy for desorption of $278\text{ kJ}\cdot\text{mol}^{-1}$ for the first silver monolayer may be derived. An Arrhenius plot derived from the leading edge of the lower temperature peak yielded an activation energy to desorption from this state of $283\text{ kJ}\cdot\text{mol}^{-1}$, which may be compared with the heat of sublimation for Ag of $254\text{ kJ}\cdot\text{mol}^{-1}$. As a confirmation of the Auger coverage calibration for this surface, it may be noted that at an initial Ag coverage of 2 monolayers, the heights of the two desorption peaks are equal.

TDS results for Ag desorption from the Pt(553) surface (Fig.5b) again indicates the presence of two desorption states. However, in contrast to the behavior found for the Pt(111)/Ag system, both peaks are present at initial coverages below 1 monolayer. At 1 monolayer the two peaks are of comparable intensity, and at 2 monolayers the lower temperature peak becomes the dominant feature. These observations indicate that silver is present as multilayer 3D crystallites, even at very low initial exposures, as would be expected from a system following a Volmer-Weber growth mechanism. The same results were obtained using a Pt(S)-[6(111)x(100)] crystal.

A series of LEED observations were made during the growth of Ag on the Pt(111) substrate. Deposition of Ag at 300 K led to a degradation in spot definition and an increase in background intensity until all diffraction features disappeared at Ag coverages >0.2 monolayers. After annealing the crystal with Ag coverages between 0.0 and ~ 0.3 monolayers, no improvement in the quality of the diffraction pattern was observed. At higher coverages, up to ~ 10 monolayers, annealing at ~ 500 K for several minutes led to a dramatic increase in the quality of the diffraction pattern. No extra order spots or spot streaking were observed at all coverages, indicating that the Ag adlayer was growing

pseudomorphically on the Pt substrate. The number of Ag atoms forming a monolayer on the Pt(111) surface is, therefore, equal to the atomic density of the Pt(111) surface (1.5×10^{15} atoms cm^{-2}).

4.2 Adsorption of CO on the Ag covered Pt(111) and Pt(533) surfaces.

The adsorption of CO on both the Pt(111) and stepped Pt surfaces has been the subject of much investigation^{6,8,9}. Briefly, thermal desorption studies reveal that CO adsorbs non-dissociatively on both the flat and stepped Pt surfaces. A single CO desorption state with a coverage dependent peak maximum centered at ~ 480 K at low coverages and at ~ 400 K at saturation coverages is observed from the Pt(111) face. An additional, higher temperature state at ~ 500 K is always observed from stepped surfaces, its intensity varying with the surface step density. This higher binding energy state is attributed to the desorption of CO molecules adsorbed at step edges.

Saturation coverage (12 L) CO desorption spectra from the Pt(111) specimen preexposed to various coverages at Ag are presented in Fig.6a. The desorption peak shapes and position are unaffected by the presence of Ag, but its peak intensity is attenuated. This effect may be quantified by plotting the integrated CO desorption yield as a function of the Ag coverage (Fig.6b). The initial slope of this plot indicates that one monolayer of Ag blocks all available CO adsorption sites.

Similar data obtained from the Pt(553) specimen are shown in Figs.7a and 7b. Again, a decrease in the total CO desorption yield with increasing Ag coverage is observed, and again, a linear decrease in CO desorption yield in direct proportion to Ag coverage is calculated. In addition, at silver coverages in the range 0.0 to 0.1 monolayers, only the lower temperature CO desorption peak is diminished in intensity. At higher silver coverages the lower binding energy CO state is attenuated more strongly than the higher temperature desorp-

tion state due to CO at the step sites. This effect is clearly discernable from Fig. 7 and is readily reproducible on other stepped Pt surfaces. From these results, it is concluded that while the step sites remain free to adsorb CO, the terrace sites are efficiently blocked by the build-up of the Ag layer.

4.3 Growth and properties of Au on Pt(111) and Pt(553)

AST plots for Au growth on both the Pt(111) and Pt(553) surfaces were determined and are presented together in Fig.8. The data derived from both the Pt(111) and Pt(553) specimens closely obey the same variations: an initial linear portion followed by a smoothly varying section to saturation value, indicating that in both cases growth proceeds by a Stranski-Krastanov mechanism. LEED observations of the growth of Au on the Pt(111) surface again gave no evidence of any ordering of the Au atoms on the Pt surface. No extra order spots or spot streaking was observed.

It should be noted that the Auger spectra of Pt and Au are so similar that resolution of their transitions was not directly possible. The relative contribution of the Au and Pt in the observed spectra was calculated by assuming that each spectrum was a linear combination of the spectra obtained from the pure Pt substrate and a surface covered with a thick (~ 10 monolayers) layer of Au. This method has been successfully used by other workers and is described in detail elsewhere.⁷

Upon heating the Au covered Pt specimen to temperatures >800 K, AES indicated that Au was rapidly removed from the surface regions. Since no desorption of Au could be detected at any Au coverage or specimen temperature by our mass spectrometer, it was concluded that the Au adlayer was dissolving into the crystal bulk at these temperatures. To prevent Au contamination of the Pt single crystal bulk, the Au adlayer was removed by Ar^+ etching during the majority of experiments with the Pt/Au system.

4.4 CO adsorption on the Au covered Pt(111) and Pt(553) surface.

Saturation coverage (12 L) CO desorption spectra from the Pt(111) specimen covered with controlled amounts of Au appear in Fig.9a. The presence of Au does not alter the position or shape of the desorption maxima, indicating that gold does not affect the binding energy of CO to the Pt surface.

Parallel data for the Pt(553) surface are shown in Figs.10a and 10b. No changes in thermal desorption peak positions are indicated. Thus the presence of gold does not alter the CO binding energy to the platinum surface, it only reduces the number of available adsorption sites. Once again as was shown in the Ag studies, the Au adlayer blocks CO adsorption sites linearly in direct proportion to coverage.

In contrast to the behavior of Ag adsorbed on stepped surfaces, no selective blocking of either the terrace or step sites was detected. It appears that Au adsorbs on both step and terrace sites in a statistical distribution.

5. Discussion

From thermal desorption studies of the Ag adlayer from the Pt specimens we determined that the Ag-Pt bond in the first monolayer was $\sim 25 \text{ kJ}\cdot\text{mol}^{-1}$ stronger ($278 \text{ kJ}\cdot\text{mol}^{-1}$) than the Ag-Ag bond ($253 \text{ kJ}\cdot\text{mol}^{-1}$) in the subsequent monolayers. It is therefore to be expected that the first monolayer of Ag deposited on the Pt substrate would spread evenly over the surface to maximize the number of Ag-Pt bonds. For the growth of Ag on the Pt(111) surface, this was found to be the case as shown by both AES studies and Ag thermal desorption results. However, the introduction of steps into the Pt surface changes the growth to a three-dimensional crystallite mechanism. From the thermal desorption studies of Ag at less than one monolayer coverage we note the appearance of two desorption peaks from stepped surfaces. These peaks can be associated with the desorption

of Ag from Ag islands as well as from clean platinum. The location of these three-dimensional Ag crystallites can be determined from the CO TDS results on the partially Ag covered stepped Pt crystal surfaces. A marked attenuation of the CO desorption peak attributed to CO molecules desorbing from the terraces of a stepped crystal surface, while not substantially altering the intensity of the peak identified with the desorption of CO from step sites, provides the evidence for the selective adsorption of Ag onto the terrace sites of the stepped surface. Thus on a partially covered Ag surface, the step Pt sites are readily available for chemisorption while terrace sites are blocked in proportion to Ag coverage. This is a surprising result indeed since studies of the adsorption of diatomic molecules (e.g. CO, H₂, O₂) on stepped Pt surfaces indicate stronger bonding and preferential adsorption or dissociation at the stepped Pt surfaces step edges.⁸ While silver does not appear to adsorb at step sites to prevent CO adsorption we cannot rule out the possibility that it may be located under the surface where it cannot be detected and does not interfere with CO chemisorption. However, thermal desorption of Ag indicates that it can be removed readily from the platinum surface and we have no evidence for its incorporation in the bulk of the platinum crystals.

The presence of submonolayer amounts of Ag or Au on the Pt crystal surfaces did not alter the observed heat of adsorption of CO at saturation CO coverages. The adsorption of CO on clean Pt surfaces has been well characterized as a non-dissociative process with a heat of adsorption that decreases with increasing CO coverage from ~ 33 kcal/mole⁻¹ to ~ 28 kcal/mole⁻¹. This is due to repulsive interactions between the adsorbed CO molecules. As the C=O bond is perpendicular to the surface the molecules that occupy a top or bridge site on the Pt(111) surface may be viewed as an array of dipoles. At closer packing dipolarization as a result of repulsive interaction of like dipoles leads to the weakening of the

metal-CO bond.⁹ The invariance of the heat of adsorption of CO at saturation coverage indicates that these same lateral interactions are maintained despite the presence of the Ag or Au. This strongly suggests that the deposited Ag or Au atoms form islands which allow the CO molecules to maintain their usual close packing on the remaining uncovered surface of platinum. In contrast, when a Au/Pt alloy is formed by allowing the deposited Au to diffuse into the surface region of the platinum, an increase in the heat of adsorption is noted, consistent with the reduced repulsive interactions between CO molecules as the concentration of platinum atom chemisorption sites is diluted by the gold atoms.¹⁰

It was not possible to determine the energetics of the Au adlayer adsorbed on the Pt substrate since no desorption of Au could be detected. Growth of gold layers on both the Pt(111) and Pt(553) surfaces proceeds via the Stranski-Krastanov mechanism. The CO coadsorption experiments indicate that Au adsorbs uniformly on the stepped Pt surfaces. It should be concluded that the repulsive effect of the platinum steps observed for Ag does not play a role in the Pt/Au system. This work is being continued by examining the adsorption and properties of Cu on the flat (111) and on stepped Pt crystal surfaces.

Acknowledgement:

This work was supported by the Director, Office of Energy Research, Office of Basic Energy Sciences, Materials Sciences Division of the U.S. Department of Energy under Contract DE-AC03-76SF00098, and a grant from the Dow Chemical Company.

References

1. V. Ponec, Catal. Rev.-Sci. Eng. 11, (1970) 41.
2. V. Ponec, Surface Sci. 80, (1979) 352.
3. W.M.H. Sachtler, Catal. Rev.-Sci. Eng. 14, (1976) 193.
4. T.E. Gallon, Surface Sci. 17, (1969) 486.
5. P. Redhead, Vacuum 12, (1962) 203.

6. D.M. Collins and W.E. Spicer, Surface Sci. 69, (1977) 85.
7. J.W.A. Sachtler, M.A. Van Hove, J.P. Biberian, and G.A. Somorjai, Surface Sci. 110 (1981) 19.
8. B. Lang, B. Joyner, and G.A. Somorjai, Proc. Roy. Soc. (Lond.) A331, (1972) 335; S. Bernasek, W. Seikhaus, and G.A. Somorjai, Phys. Rev. Lett. 30 (1973) 1202; S. Ceyer, R. Gale, S. Bernasek, and G.A. Somorjai, J. Chem. Phys. 64 (1976) 1934; D. Blakely and G.A. Somorjai, J. Catal. 42 (1976) 141.
9. G. Ertl, M. Neumann, K.M. Streit, Surf. Sci. 64 (1977) 393; H. Hopster and H. Ibach, Surface Sci. 77 (1978) 109; A. Crossley and D.A. King, Surf. Sci. 95 (1980) 131.
10. J.W.A. Sachtler and G.A. Somorjai, (to be published).

Figure Captions

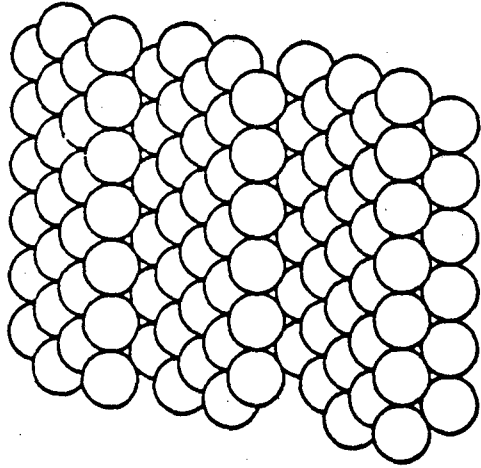
- Fig.1 Schematic representations of the fcc (111) and fcc (553) surfaces.
- Fig.2 Growth mechanisms for thin films on metal substrates together with the expected variation in the Auger signal of both substrate and adsorbate. G.E. Rhead, J. Vac. Sci. Technol. 13 (1976) 603.
- Fig.3 (A) Auger spectrum of clean Pt(111).
(B) Auger spectrum of the surface covered with ~ 0.8 monolayers of silver.
- Fig.4 Auger uptake curve for silver deposited on (a) Pt(111), (b) Pt(553).
- Fig.5 Silver (AMU 107) thermal desorption spectra from Pt surface as a function of Ag coverage. (a) Pt(111) and (b) Pt(553).
- Fig.6 (A) Carbon monoxide (AMU 28) thermal desorption spectra from the Pt(111) surface as a function of Ag coverage
(B) Normalized carbon monoxide thermal desorption yield as a function of Ag coverage.
- Fig.7 (A) Carbon monoxide (AMU 28) thermal desorption spectra from the Pt(553) surface.
(B) Normalized carbon monoxide thermal desorption yield as a function of Ag coverage.
- Fig.8 Auger uptake curve for gold deposited on (a) Pt(111) (b) Pt(553).

Fig.9 (A) Carbon monoxide (AMU 28) thermal desorption spectra from the Pt(111) surface as a function of Au coverage.

(B) Normalized carbon monoxide thermal desorption yield as a function of Au coverage.

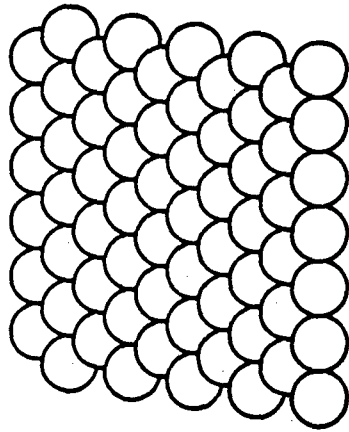
Fig.10 (A) Carbon monoxide (AMU 28) thermal desorption spectra from the Pt(553) surface as a function of Au coverage.

(B) Normalized carbon monoxide thermal desorption yield as a function of Au coverage.



fcc (553)

XBL 8111-12652



fcc (111)

Fig. 1

THIN FILM GROWTH MECHANISMS

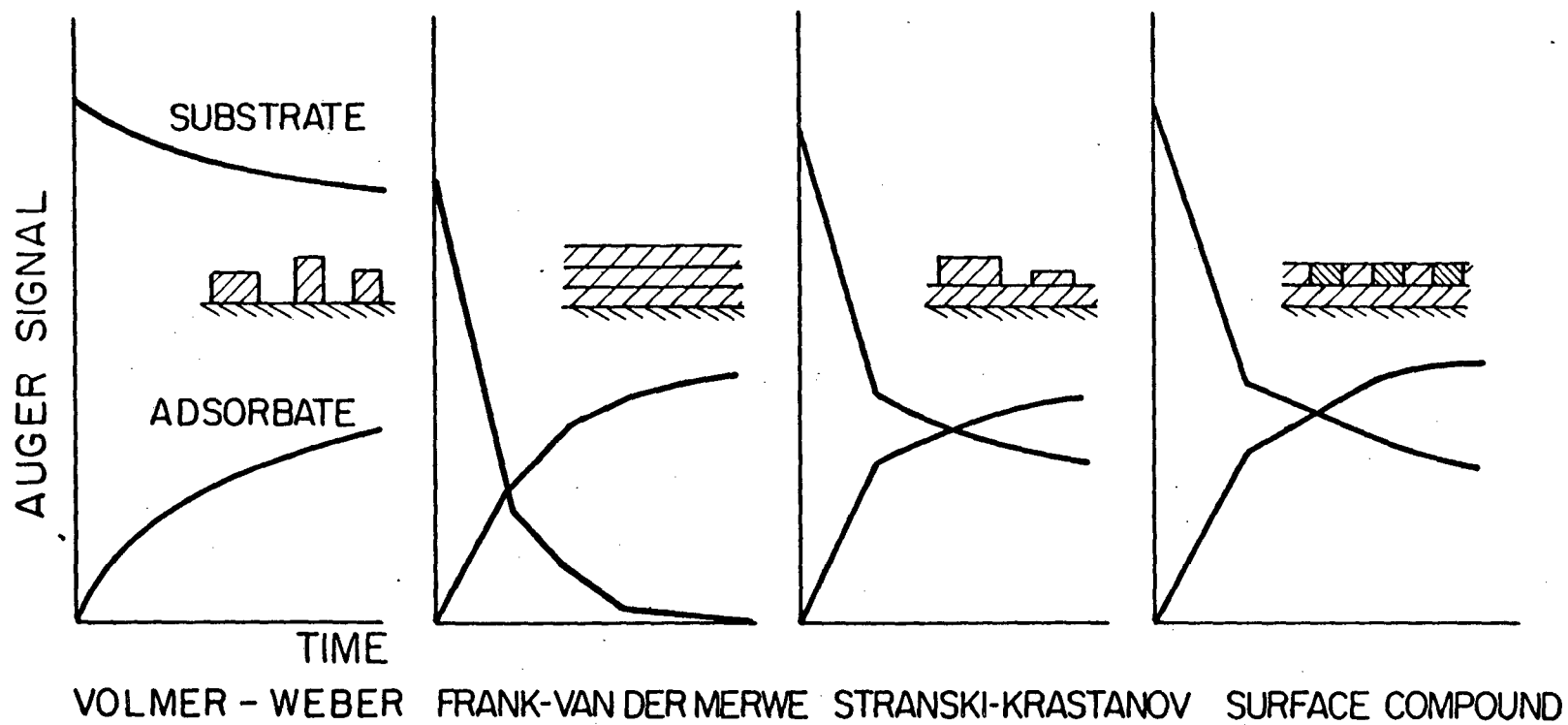


Fig. 2

XBL 814-5523

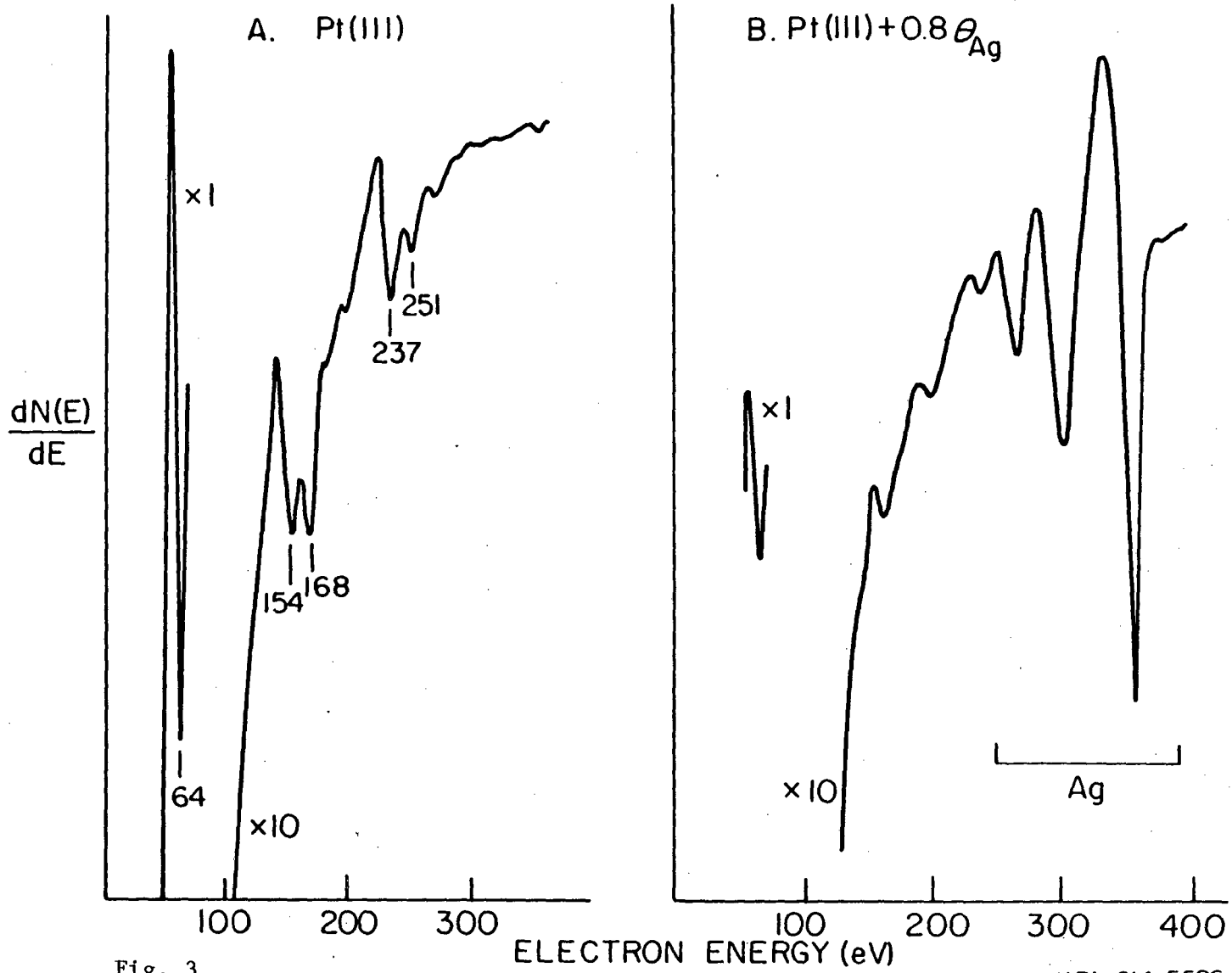
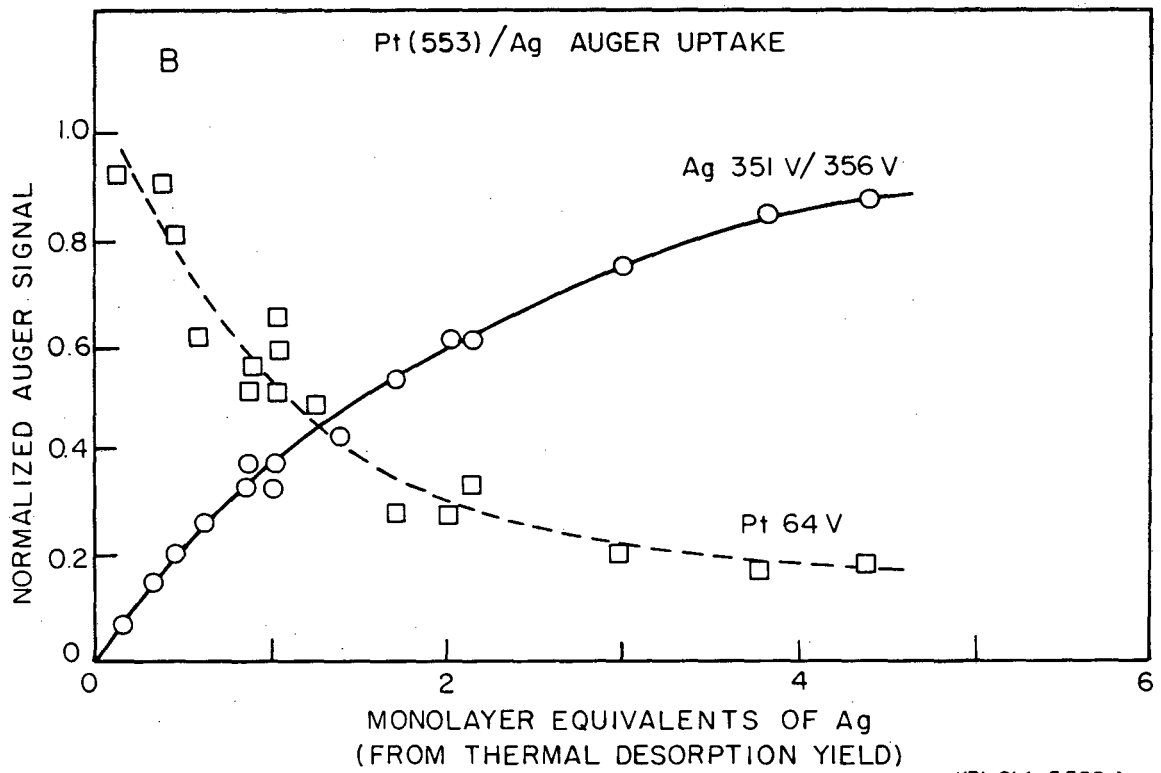
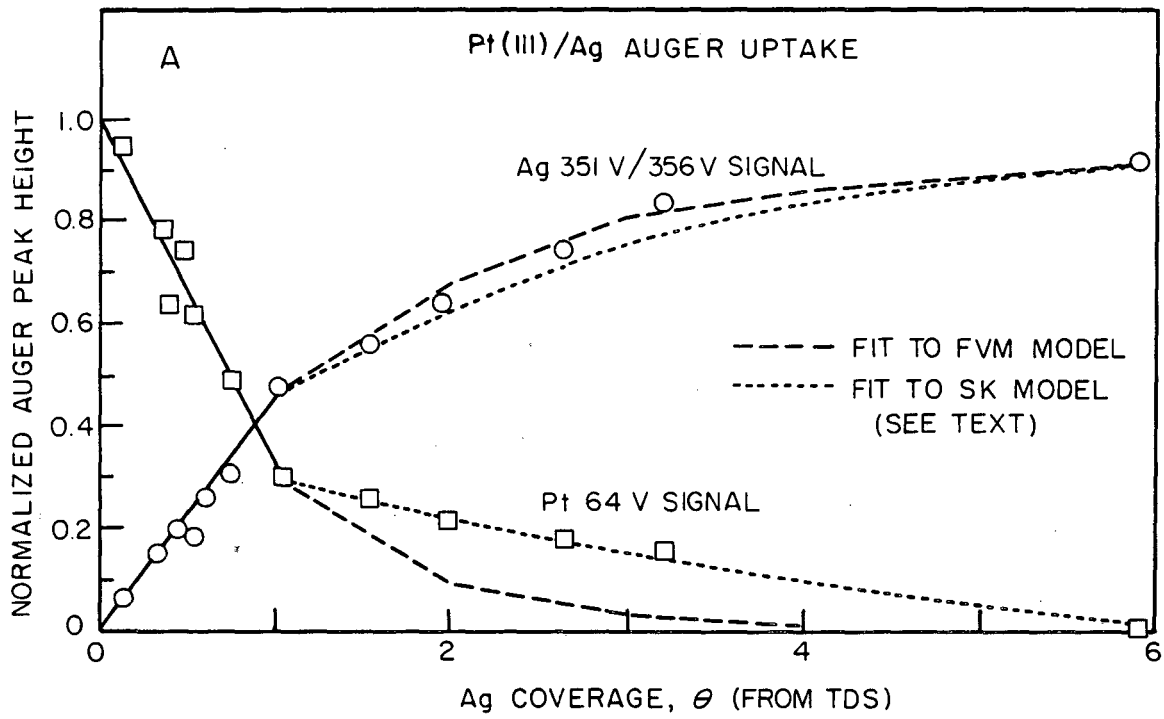


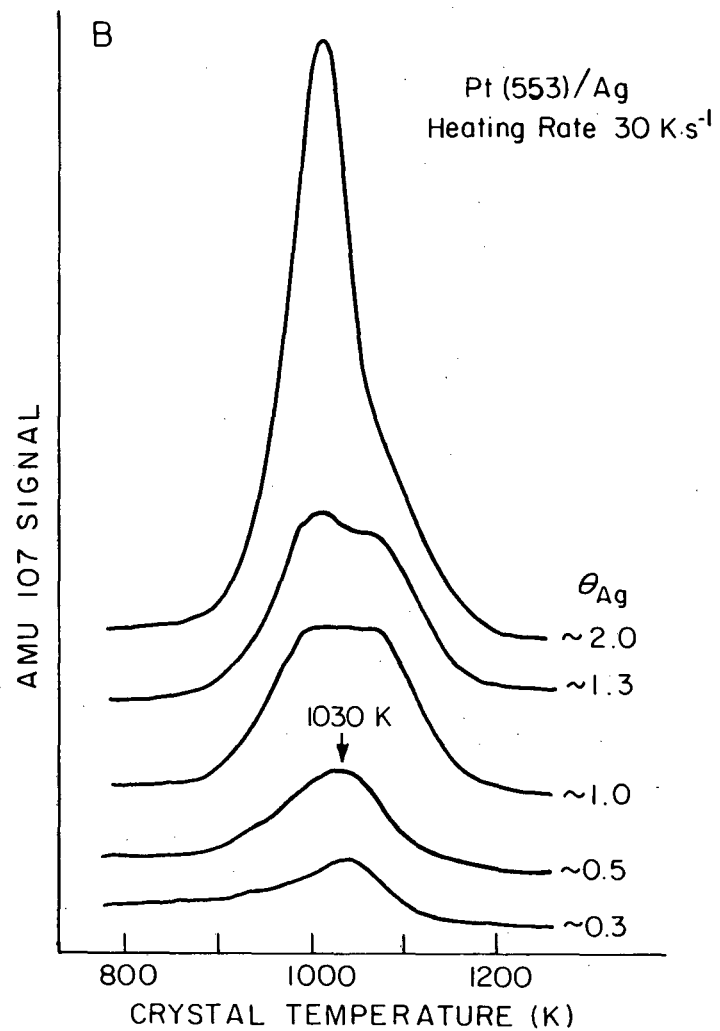
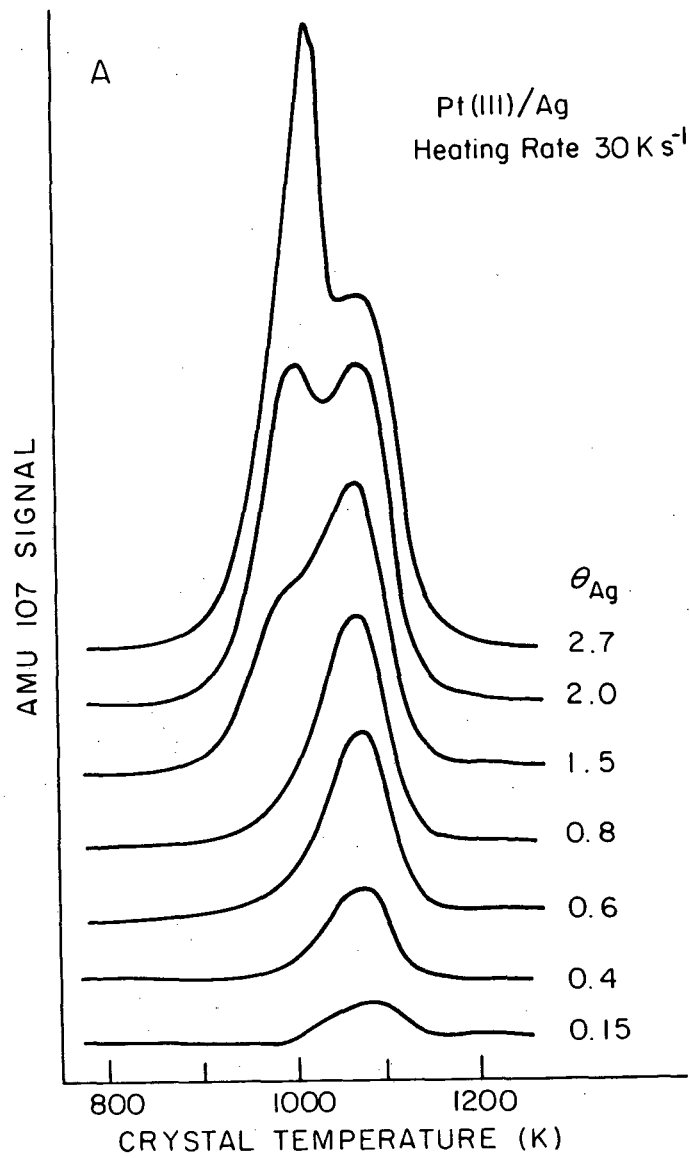
Fig. 3

XBL 814-5526



XBL 814-5530 A

Fig. 4



XBL 814-5522A

Fig. 5

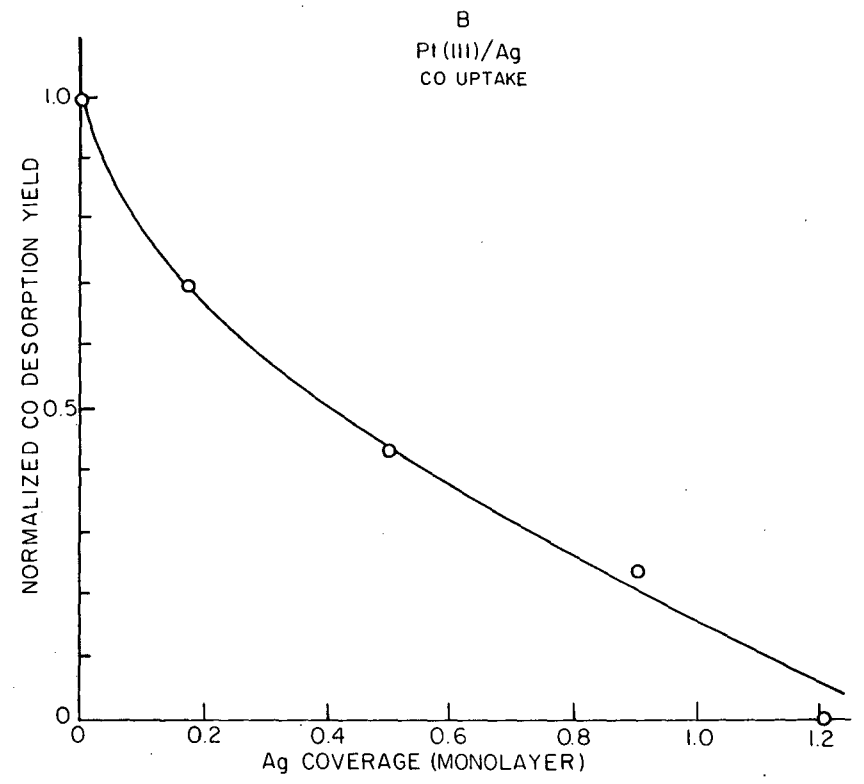
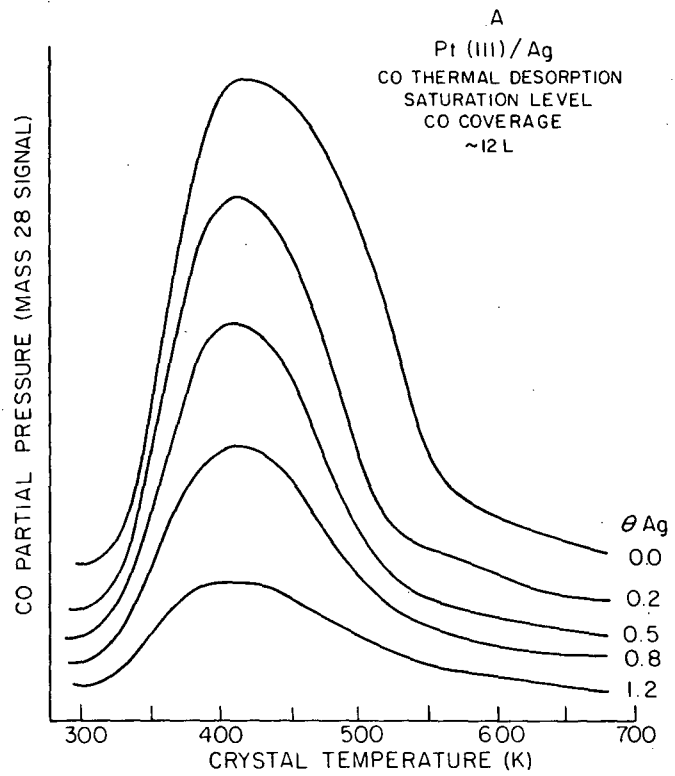


Fig. 6

XBL 823-5450

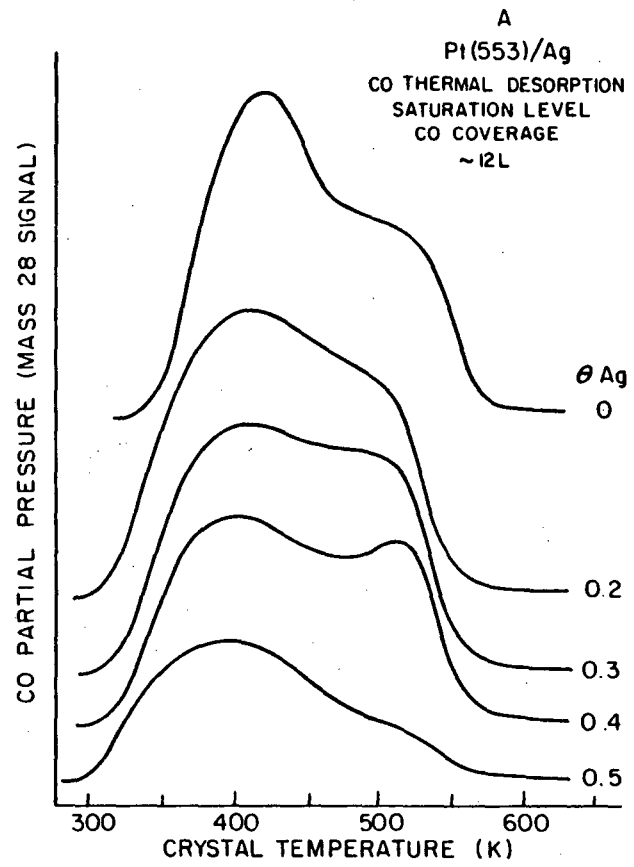
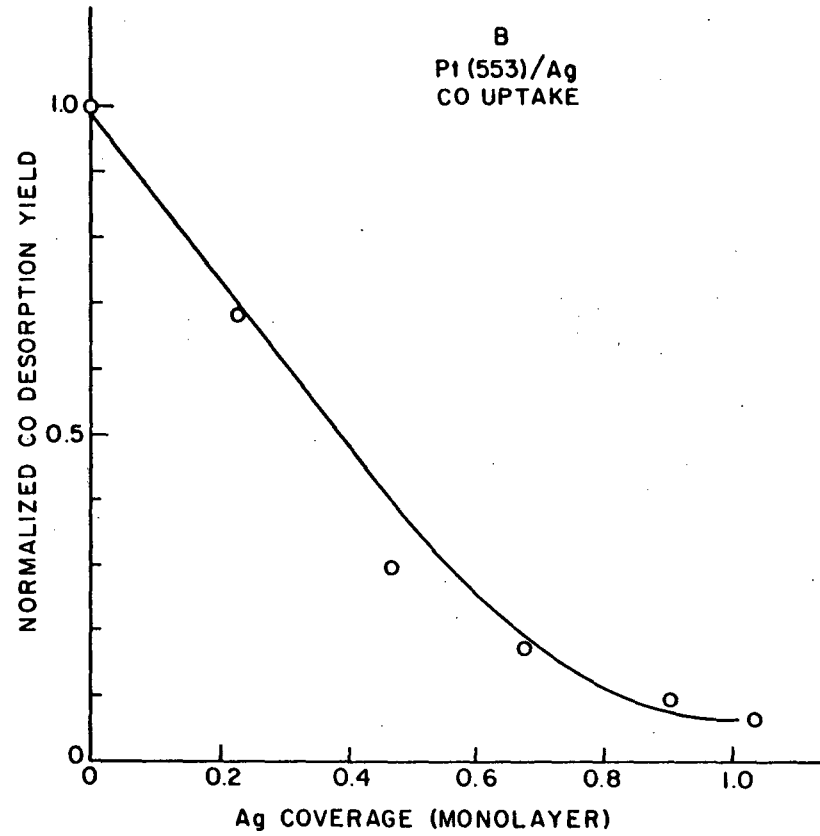
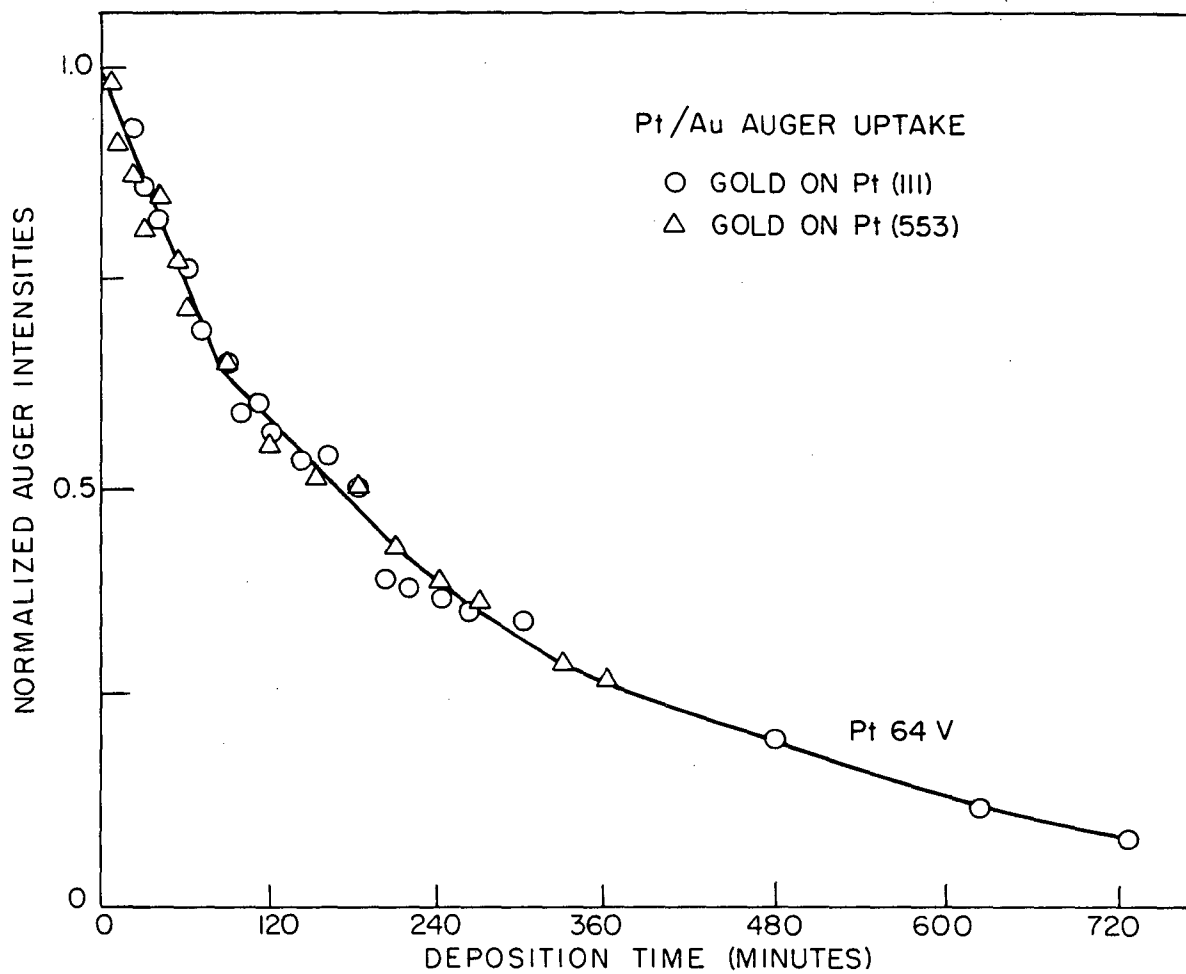


Fig. 7



XBL8111-6941



XBL 814-5538

Fig. 8

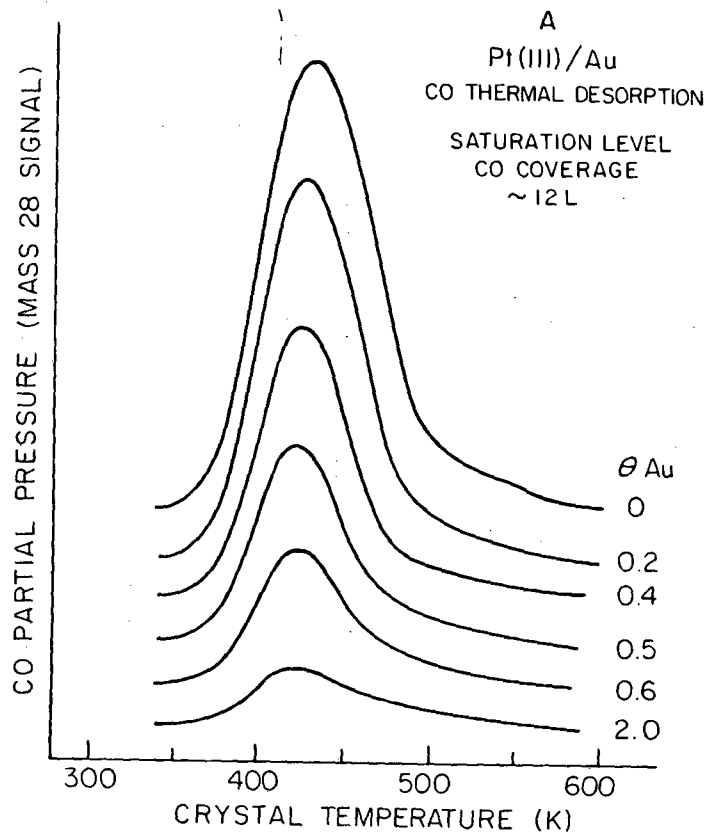
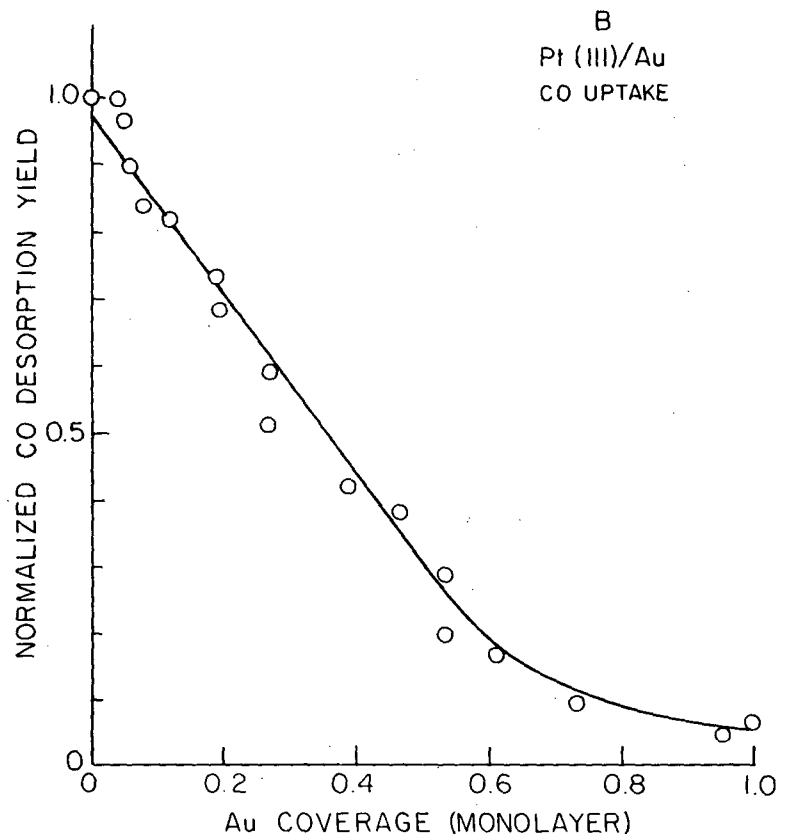


Fig. 9



XBL8111-6939

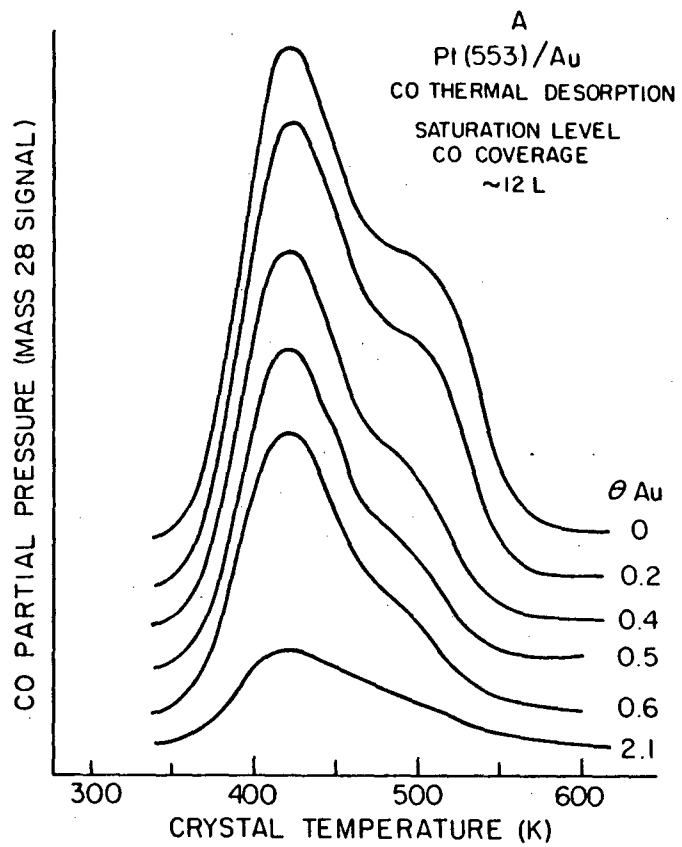
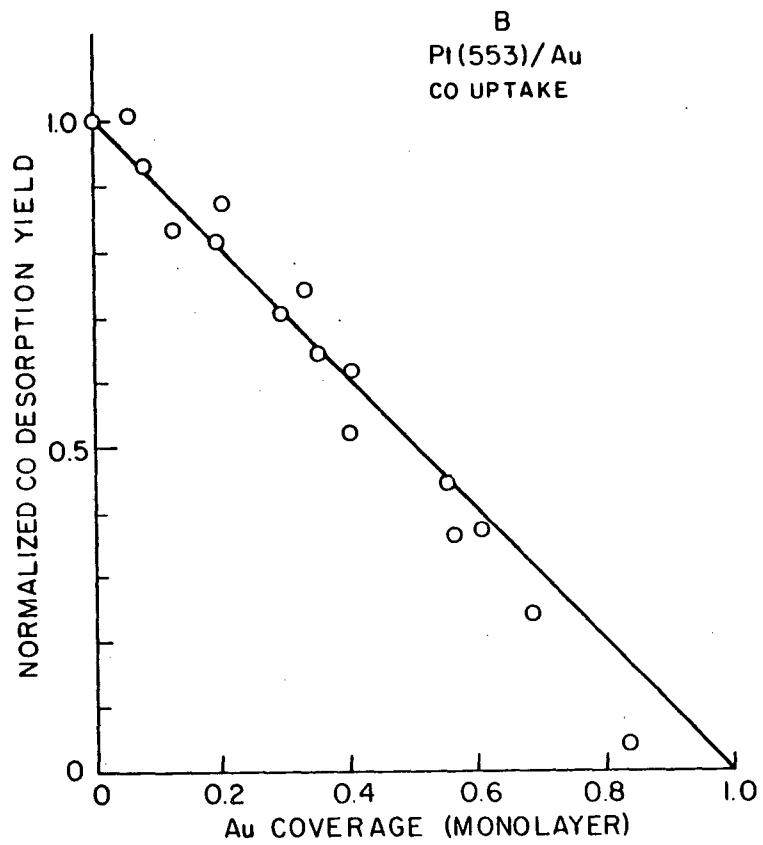


Fig. 10



XBL 8111-6940

This report was done with support from the Department of Energy. Any conclusions or opinions expressed in this report represent solely those of the author(s) and not necessarily those of The Regents of the University of California, the Lawrence Berkeley Laboratory or the Department of Energy.

Reference to a company or product name does not imply approval or recommendation of the product by the University of California or the U.S. Department of Energy to the exclusion of others that may be suitable.

TECHNICAL INFORMATION DEPARTMENT
LAWRENCE BERKELEY LABORATORY
UNIVERSITY OF CALIFORNIA
BERKELEY, CALIFORNIA 94720